

Supporting Information

Excitation Wavelength Reliant Light Induced Energy and Electron Processes in Pyrene and Naphthalene Functionalized Dual-Dye Integrated Polyaromatic Azaborondipyrromethenes

Boligorla Anjaiah,^a Manne Naga Rajesh,^{b,c} Lingamallu Giribabu,^{*b,c} Raghu Chitta^{*a}

^a*Artificial Photosynthesis Laboratory, Department of Chemistry, National Institute of Technology Warangal, Hanamkonda – 506004, Telangana, India.*

^b*Polymers & Functional Materials Division, CSIR-Indian Institute of Chemical Technology, Tarnaka, Hyderabad-500007, Telangana, India.*

^c*Academy of Scientific and Innovative Research, Ghaziabad, 201002, India.*

Sl. No.	Table of Contents	Page No.
Fig. S1	¹ H NMR spectrum of (<i>E</i>)-1-(naphthalen-1-yl)-3-(pyren-1-yl)prop-2-en-1-one (1a) in CDCl ₃ .	S4
Fig. S2	ESI-MS spectrum of (<i>E</i> -1-(naphthalen-1-yl)-3-(pyren-1-yl)prop-2-en-1-one (1a) in methanol.	S4
Fig. S3	¹ H NMR spectrum of (<i>E</i> -1-phenyl-3-(pyren-1-yl)prop-2-en-1-one (2a) in CDCl ₃ .	S5
Fig. S4	ESI-MS of (<i>E</i> -1-phenyl-3-(pyren-1-yl)prop-2-en-1-one (2a) in methanol.	S5
Fig. S5	¹ H NMR spectrum of 1-(Naphthalen-1-yl)-4-nitro-3-(pyren-1-yl)butan-1-one (1b) in CDCl ₃ .	S6
Fig. S6	ESI-MS of 1-(Naphthalen-1-yl)-4-nitro-3-(pyren-1-yl)butan-1-one (1b) in methanol.	S6
Fig. S7	¹ H NMR spectrum of 4-Nitro-1-phenyl-3-(pyren-1-yl)butan-1-one (2b) in CDCl ₃ .	S7
Fig. S8	ESI-MS of 4-Nitro-1-phenyl-3-(pyren-1-yl)butan-1-one (2b) in methanol.	S7
Fig. S9	¹ H NMR spectrum of (<i>Z</i>)-5-(naphthalen-1-yl)-N-(5-(naphthalen-1-yl)-3-(pyren-1-yl)-1H-pyrrol-2-yl)-3-(pyren-1-yl)-2H-pyrrol-2-imine (1c) in CDCl ₃ .	S8
Fig. S10	ESI-MS spectrum of (<i>Z</i>)-5-(naphthalen-1-yl)-N-(5-(naphthalen-1-yl)-3-(pyren-1-yl)-1H-pyrrol-2-yl)-3-(pyren-1-yl)-2H-pyrrol-2-imine (1c) in methanol.	S8
Fig. S11	¹ H NMR spectrum of (<i>Z</i>)-5-phenyl-N-(5-phenyl-3-(pyren-1-yl)-1H-pyrrol-2-yl)-3-(pyren-1-yl)-2H-pyrrol-2-imine (2c) in CDCl ₃ .	S9
Fig. S12	ESI-MS spectrum of (<i>Z</i>)-5-phenyl-N-(5-phenyl-3-(pyren-1-yl)-1H-pyrrol-2-yl)-3-(pyren-1-yl)-2H-pyrrol-2-imine (2c) in methanol.	S9
Fig. S13	¹ H NMR spectrum of 4,4-Difluoro-1,7-di-(pyren-1-yl)-3,5-di(1-naphthyl)-4-bora-3a, 4a, 8-triaza-s-indacene (1) in CDCl ₃ .	S10
Fig. S14	ESI-MS of 4,4-Difluoro-1,7-di (pyren-1-yl)-3,5-di(1-naphthyl)-4-bora-3a, 4a, 8-triaza-s-indacene (1) in methanol.	S10
Fig. S15	¹ H NMR spectrum of 4,4-Difluoro-1,7-di-(pyren-1-yl)-3,5-di(phenyl)-4-bora-3a, 4a, 8-triaza-s-indacene (2) in CDCl ₃ .	S11
Fig. S16	ESI-MS of 4,4-Difluoro-1,7-di-(pyren-1-yl)-3,5-di(phenyl)-4-bora-3a, 4a, 8-triaza-s-indacene (2) in methanol.	S11
Fig. S17	¹¹ B NMR spectrum of 4,4-Difluoro-1,7-di (pyren-1yl)-3,5-di(1-naphthyl)-4-bora-3a, 4a, 8-triaza-s-indacene (1) in CDCl ₃ .	S12
Fig. S18	¹⁹ F spectrum of 4,4-Difluoro-1,7-di (pyren-1yl)-3,5-di(1-naphthyl)-4-bora-3a, 4a, 8-triaza-s-indacene (1) in CDCl ₃ .	S12
Fig. S19	¹⁹ F NMR spectrum of 4,4-Difluoro-1,7-di-(pyren-1-yl)-3,5-di(phenyl)-4-bora-3a, 4a, 8-triaza-s-indacene (2) in CDCl ₃ .	S13
Fig. S20	Cyclic voltammetry of 1 , 2 , 3 , and TABPY in dichloromethane containing 0.1 M (n-C ₄ H ₉) ₄ NClO ₄ , with the concentrations of the compounds held at 1 mM; scan rate = 100 mV s ⁻¹ .	S14

Fig. S21	Steady-state ((a) & (b) absorption and ((c): λ_{ex} : 275 nm & (d): λ_{ex} : 335 nm) emission spectra of naphthalene (Naph) and pyrene in dichloromethane (DCM).	S15
Fig. S22	Overlay of the steady-state emission spectrum of naphthalene (Naph) and absorption spectrum of TBAPY .	S16
Fig. S23	Emission spectra of equiabsorbing solutions of 1 , 2 , 3 and the control compounds, naphthalene (Naph), pyrene, and 1,3, 5, 7-tetratolyl-azaborondipyrromethene (TBAPY) in hexanes.	S17
Fig. S24	Emission spectra of equiabsorbing solutions of 1 , 2 , 3 and the control compounds, naphthalene (Naph), pyrene, and 1,3, 5, 7-tetratolyl-azaborondipyrromethene (TBAPY) in hexanes, dichloromethane (DCM), and acetonitrile (ACN) displaying the scattering peaks.	S18
Fig. S25	Energy level diagram showing (a) photo-induced electron transfer in 2 and (b) photo-induced energy transfer in 3 in three solvents, hexanes, DCM, and ACN.	S19
Fig. S26	Fluorescence decay curves of (a & d) naphthalene (Naph), 1 , and 3 ($\lambda_{\text{ex}} = 275$ nm), (b & e) pyrene, 1 and 2 ($\lambda_{\text{ex}} = 335$ nm), and (c & f) 1,3, 5, 7-tetratolyl-azaborondipyrromethene (TBAPY), 1 , 2 , and 3 ($\lambda_{\text{ex}} = 635$ nm) in hexanes and acetonitrile respectively.	S20

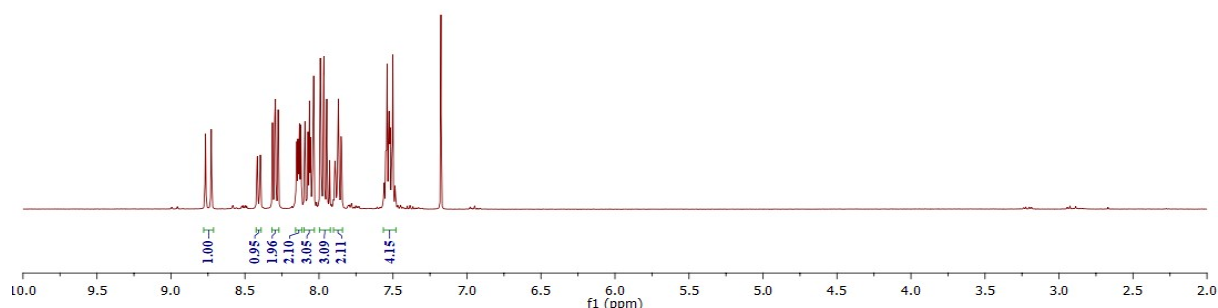
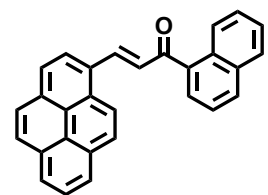


Fig. S1. ¹H NMR spectrum of (*E*)-1-(Naphthalen-1-yl)-3-(pyren-1-yl)prop-2-en-1-one (**1a**) in CDCl_3 .

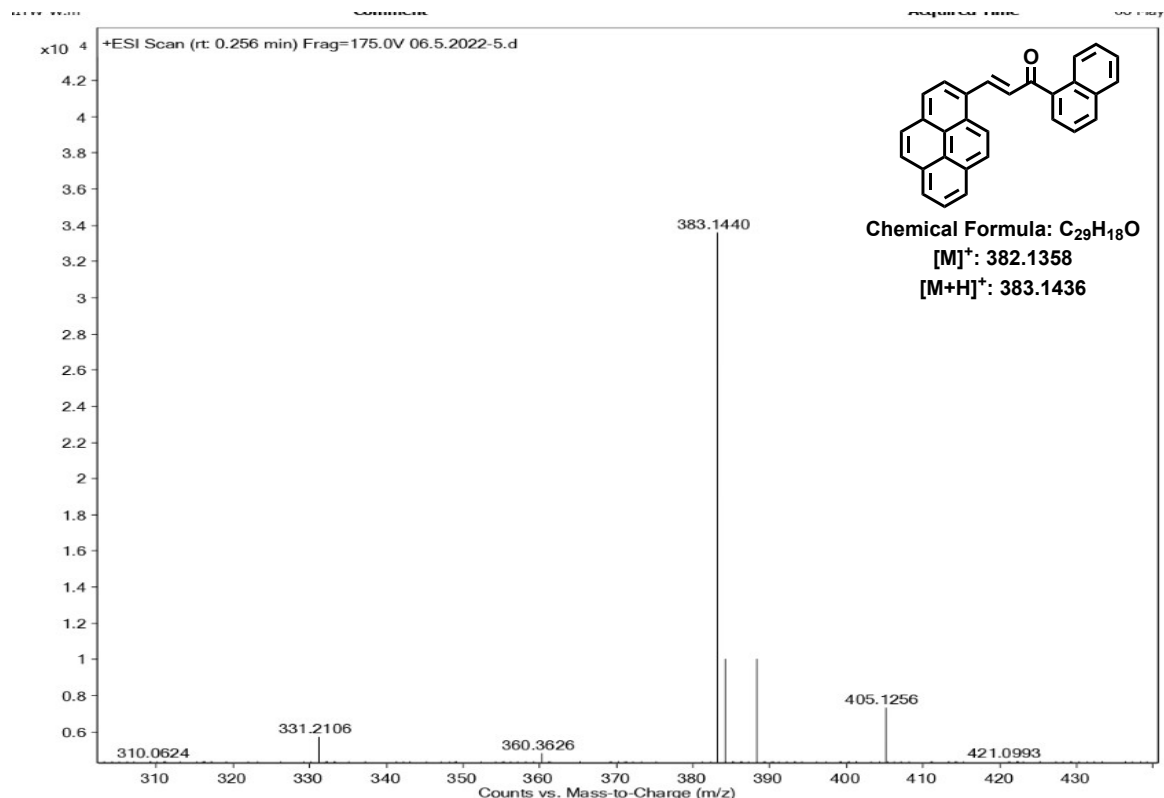


Fig. S2. ESI-MS spectrum of (*E*)-1-(Naphthalen-1-yl)-3-(pyren-1-yl)prop-2-en-1-one (**1a**) in methanol.

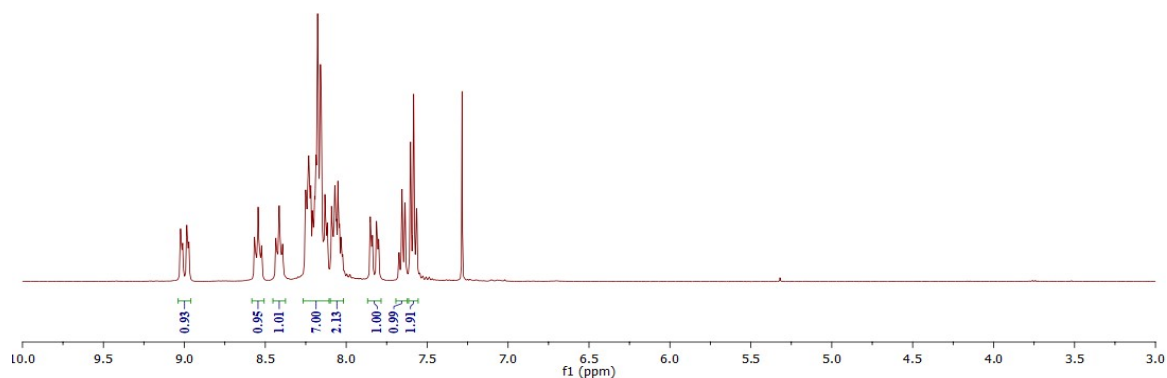
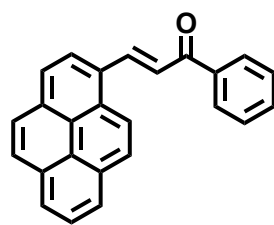


Fig. S3. ¹H NMR spectrum of (E)-1-Phenyl-3-(pyren-1-yl)prop-2-en-1-one (**2a**) in CDCl₃.

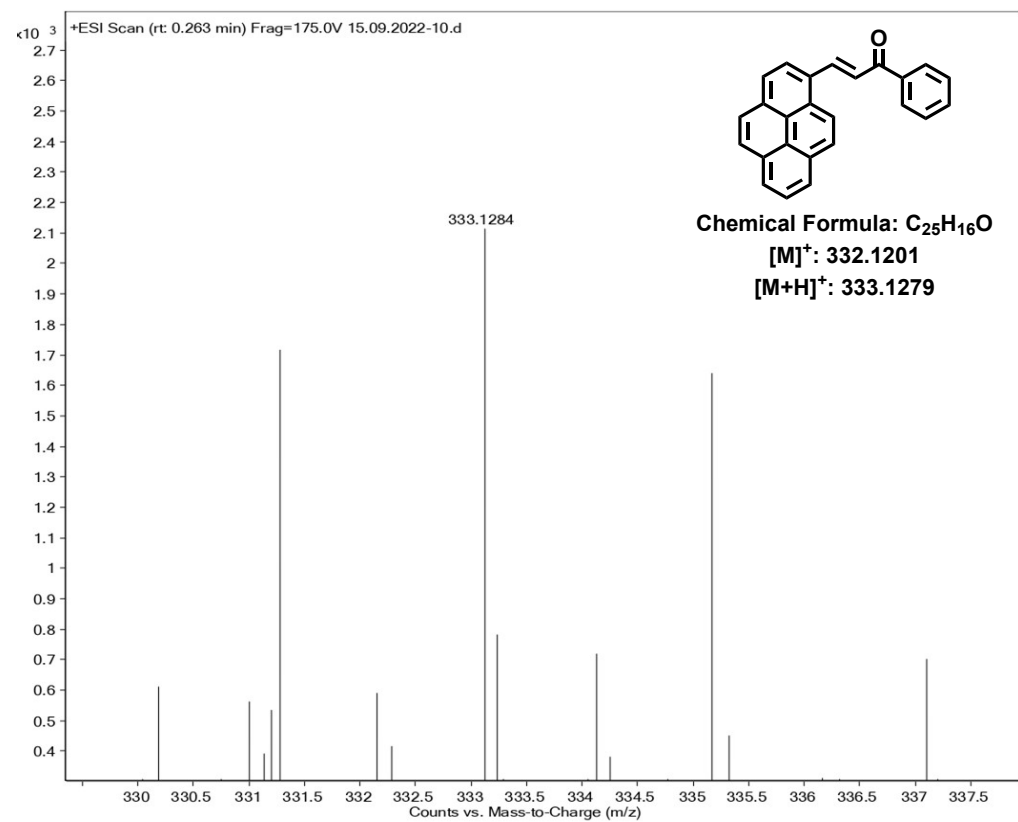


Fig. S4. ESI-MS of (E)-1-Phenyl-3-(pyren-1-yl)prop-2-en-1-one (**2a**) in methanol.

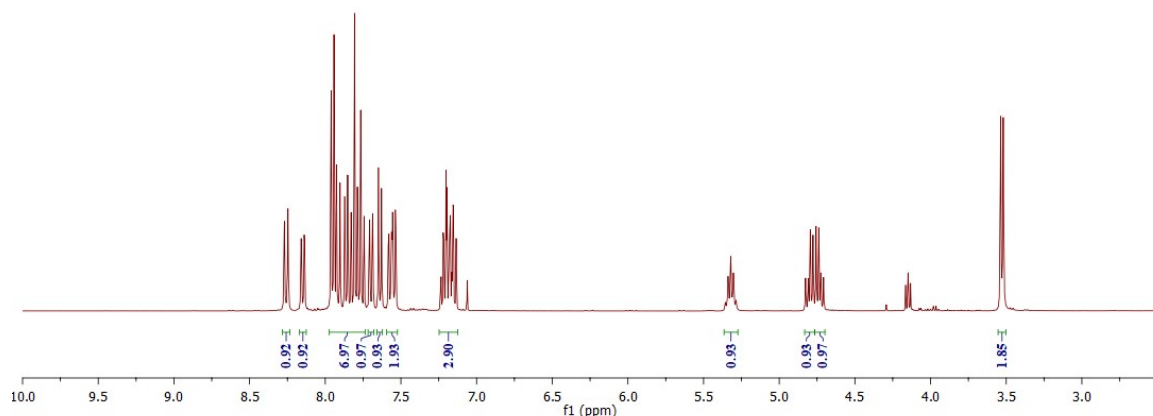
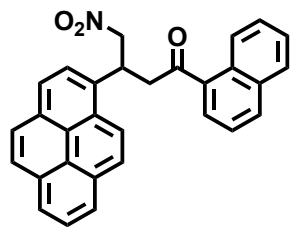


Fig. S5. ¹H NMR spectrum of 1-(Naphthalen-1-yl)-4-nitro-3-(pyren-1-yl)butan-1-one (**1b**) in CDCl_3 .

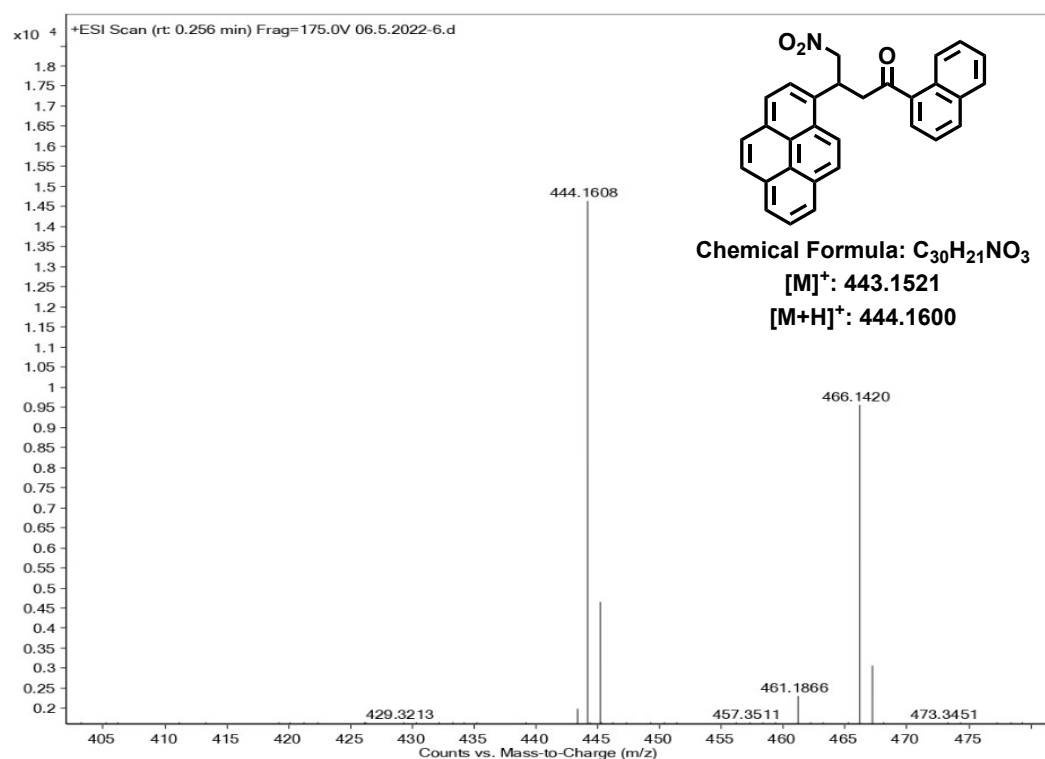


Fig. S6. ESI-MS of 1-(Naphthalen-1-yl)-4-nitro-3-(pyren-1-yl)butan-1-one (**1b**) in methanol.

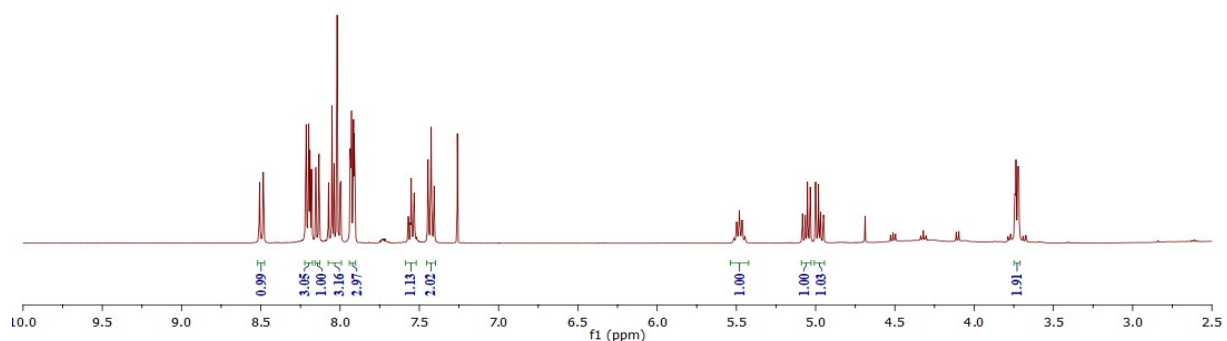
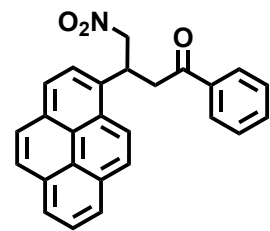


Fig. S7. ^1H NMR spectrum of 4-Nitro-1-phenyl-3-(pyren-1-yl)butan-1-one (**2b**) in CDCl_3 .

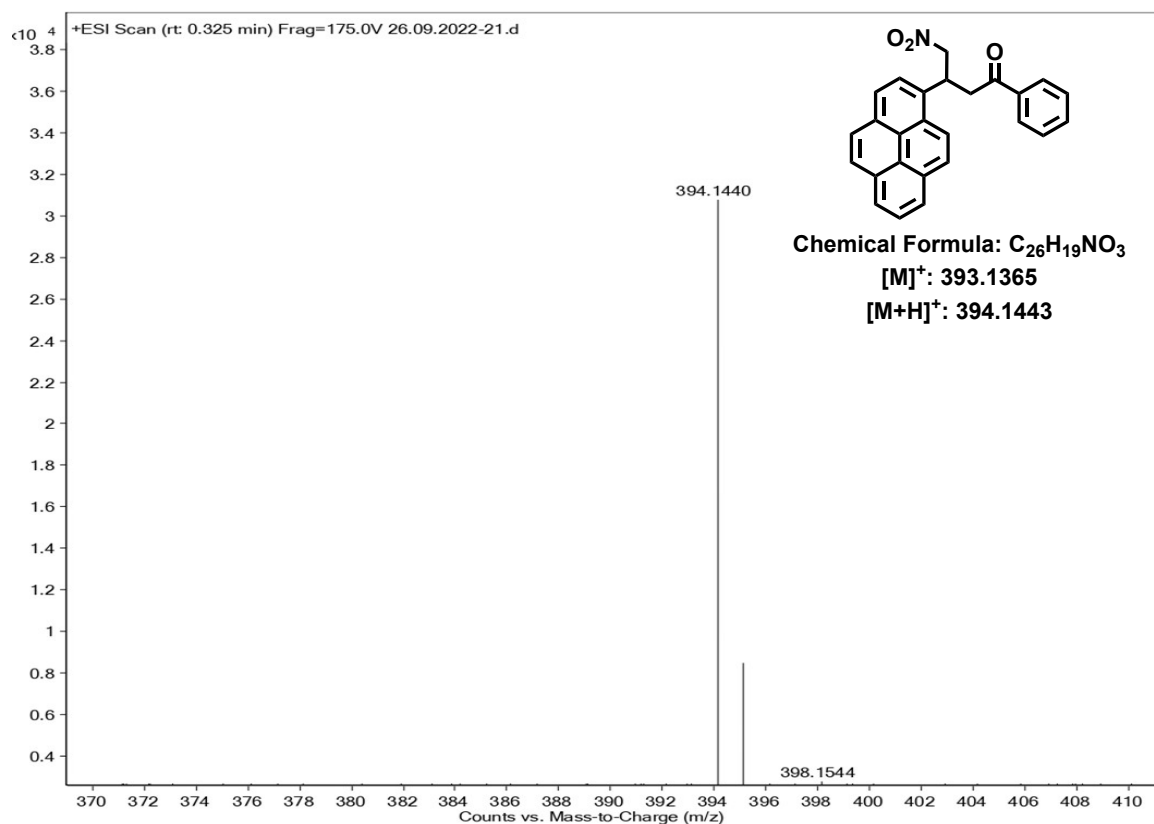


Fig. S8. ESI-MS of 4-Nitro-1-phenyl-3-(pyren-1-yl)butan-1-one (**2b**) in methanol.

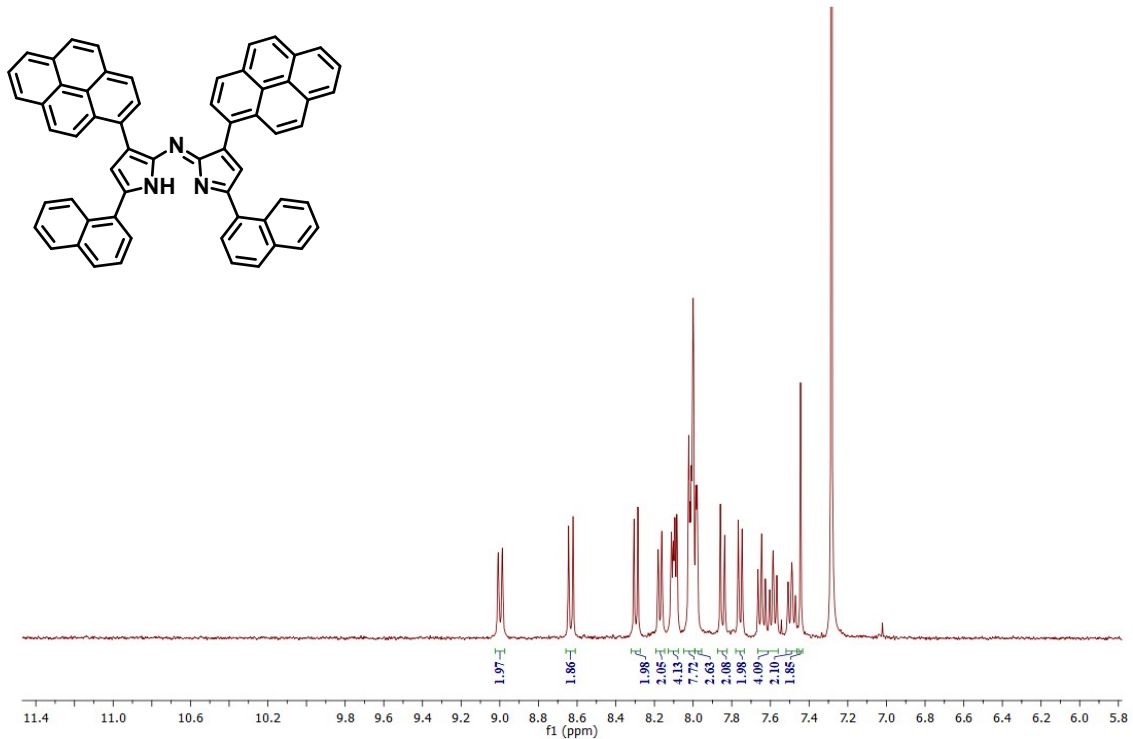


Fig. S9. ¹H NMR spectrum of (Z)-5-(Naphthalen-1-yl)-N-(5-(naphthalen-1-yl)-3-(pyren-1-yl)-1H-pyrrol-2-yl)-3-(pyren-1-yl)-2H-pyrrol-2-imine (**1c**) in CDCl₃.

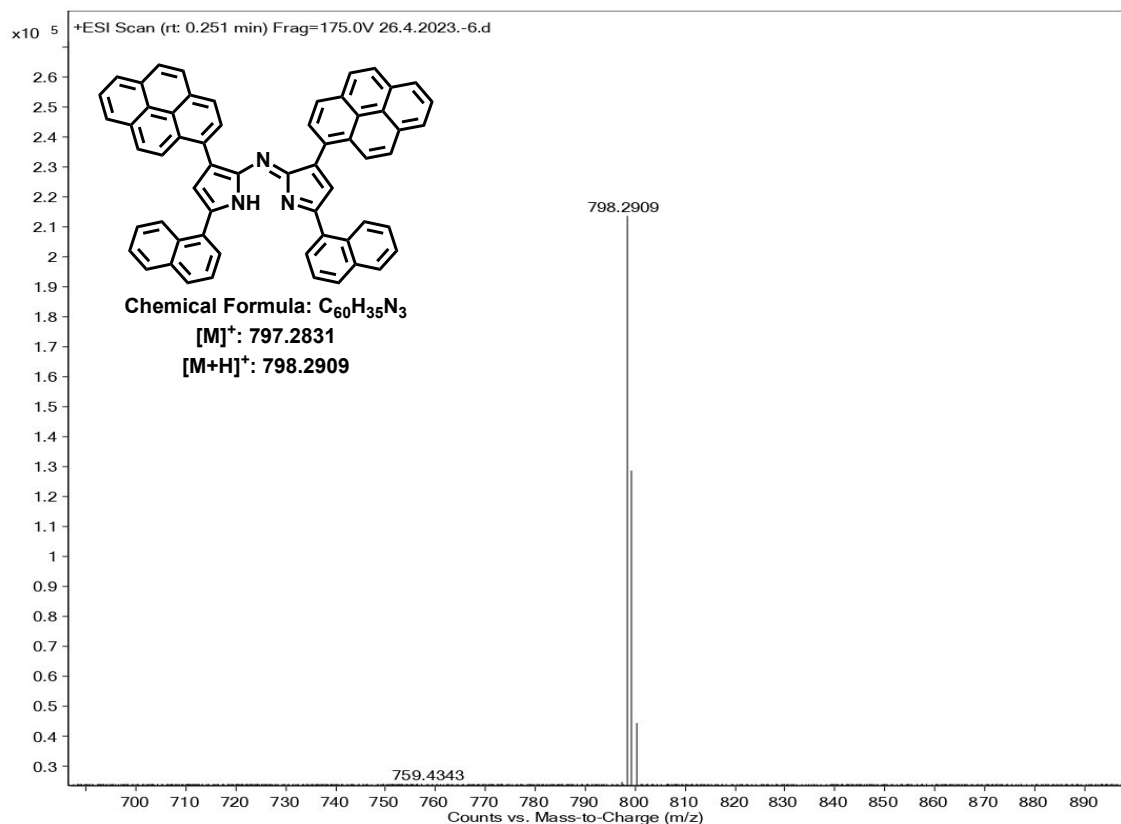


Fig. S10. ESI-MS spectrum of (Z)-5-(Naphthalen-1-yl)-N-(5-(naphthalen-1-yl)-3-(pyren-1-yl)-1H-pyrrol-2-yl)-3-(pyren-1-yl)-2H-pyrrol-2-imin (**1c**) in methanol.

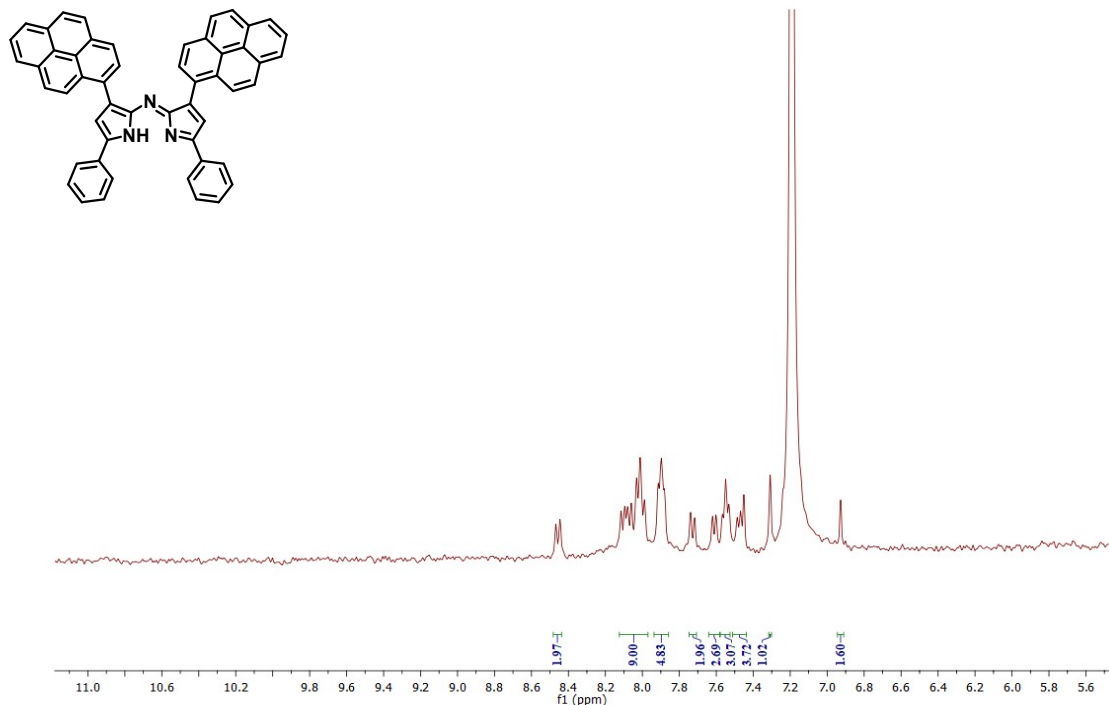


Fig. S11. ¹H NMR spectrum of (Z)-5-Phenyl-N-(5-phenyl-3-(pyren-1-yl)-1H-pyrrol-2-yl)-3-(pyren-1-yl)-2H-pyrrol-2-imine (**2c**) in CDCl₃.

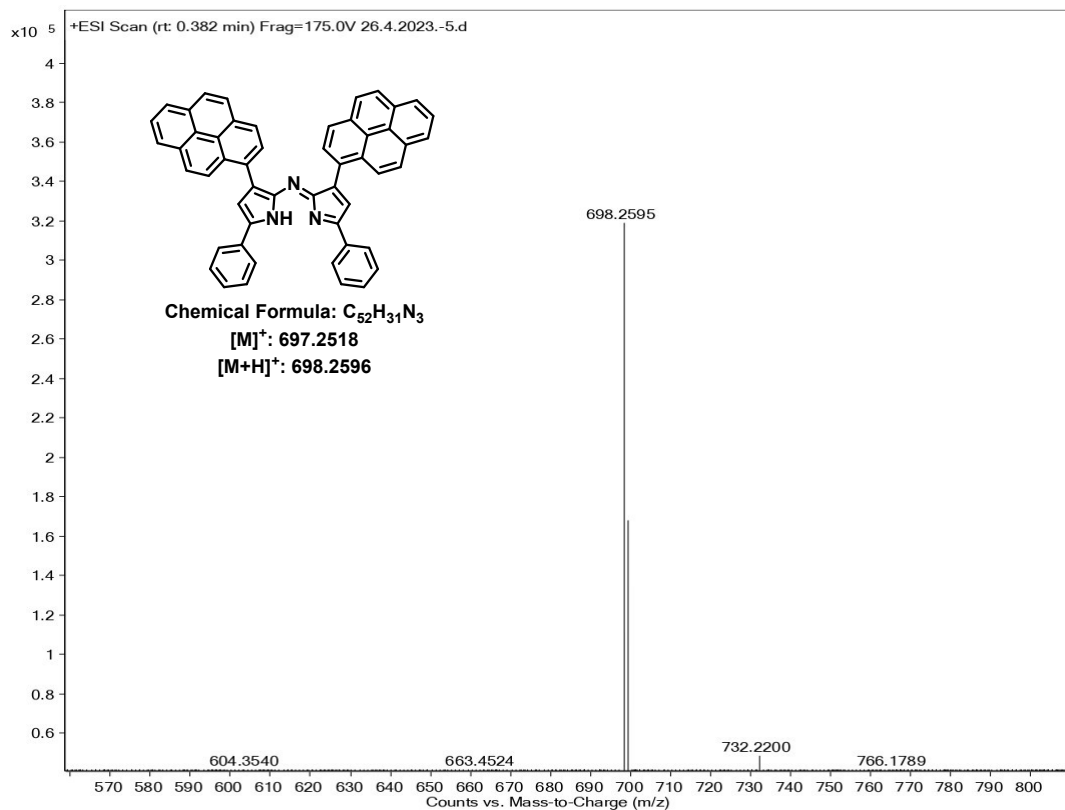


Fig. S12. ESI-MS spectrum of (Z)-5-phenyl-N-(5-phenyl-3-(pyren-1-yl)-1H-pyrrol-2-yl)-3-(pyren-1-yl)-2H-pyrrol-2-imine (**2c**) in methanol.

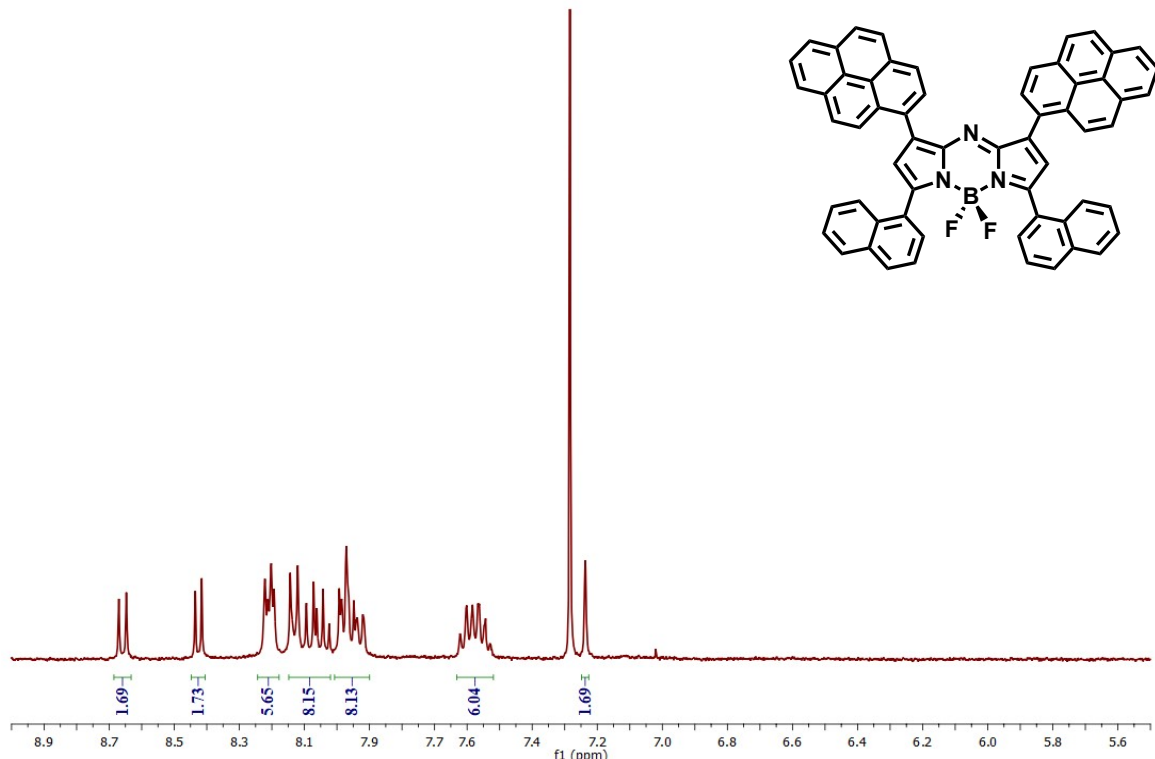


Fig. S13. ¹H NMR spectrum of 4,4-Difluoro-1,7-di-(pyren-1-yl)-3,5-di(1-naphthyl)-4-bora-3a, 4a, 8-triaza-s-indacene (**1**) in CDCl₃.

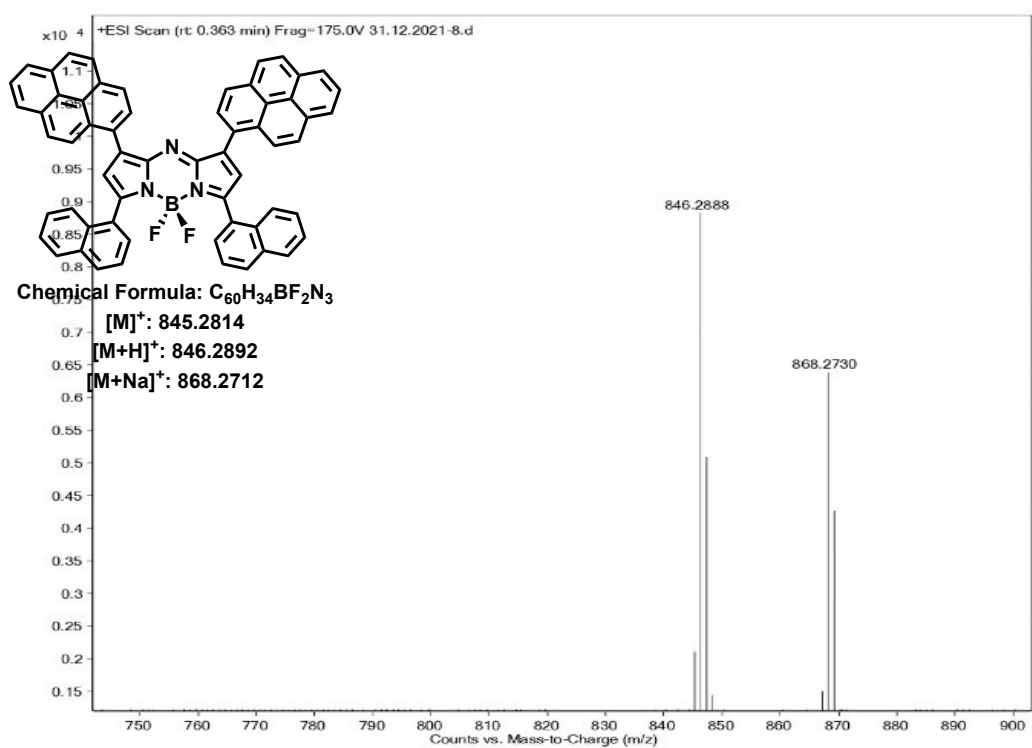


Fig. S14. ESI-MS of 4,4-Difluoro-1,7-di (pyren-1-yl)-3,5-di-(1-naphthyl)-4-bora-3a, 4a, 8-triaza-s-indacene (**1**) in methanol.

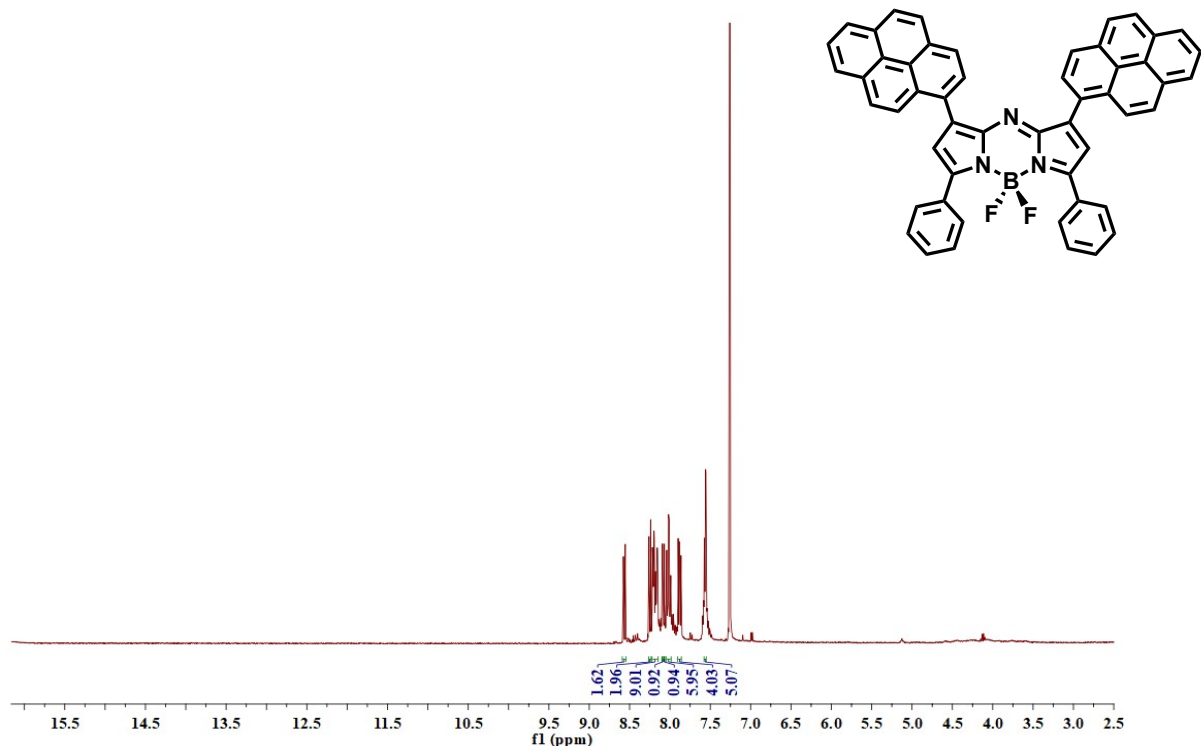


Fig. S15. 4,4-Difluoro-1,7-di-(pyren-1-yl)-3,5-di(phenyl)-4-bora-3a, 4a, 8-triaza-s-indacene (**2**) in CDCl_3 .

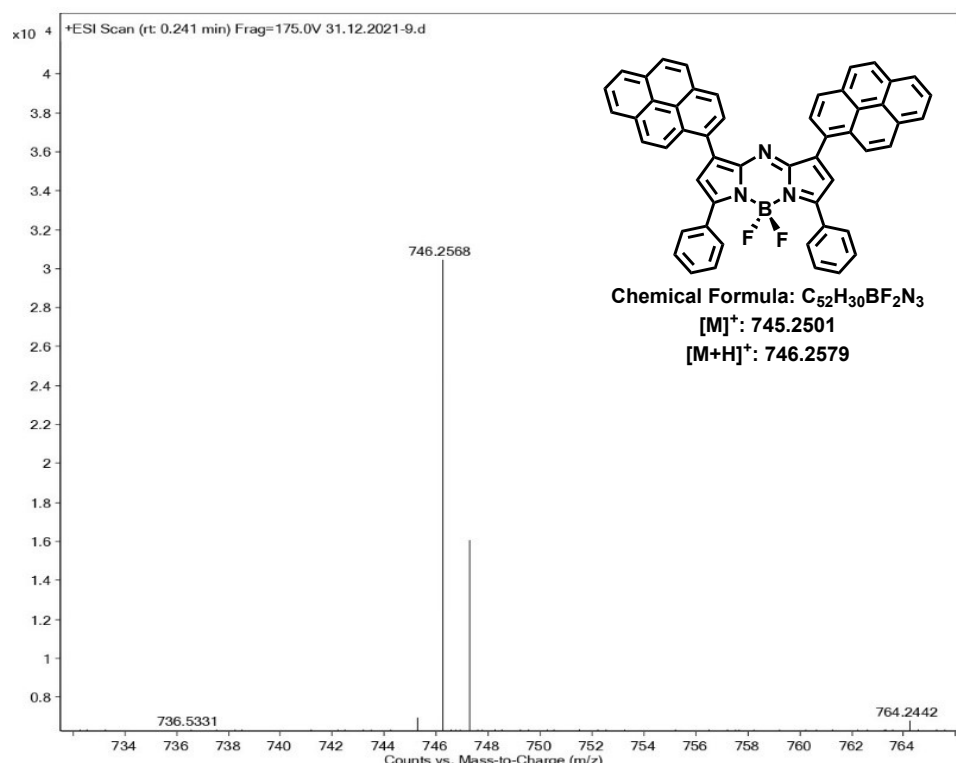


Fig. S16. ESI-MS of 4,4-Difluoro-1,7-di-(pyren-1-yl)-3,5-di(phenyl)-4-bora-3a, 4a, 8-triaza-s-indacene (**2**) in methanol.

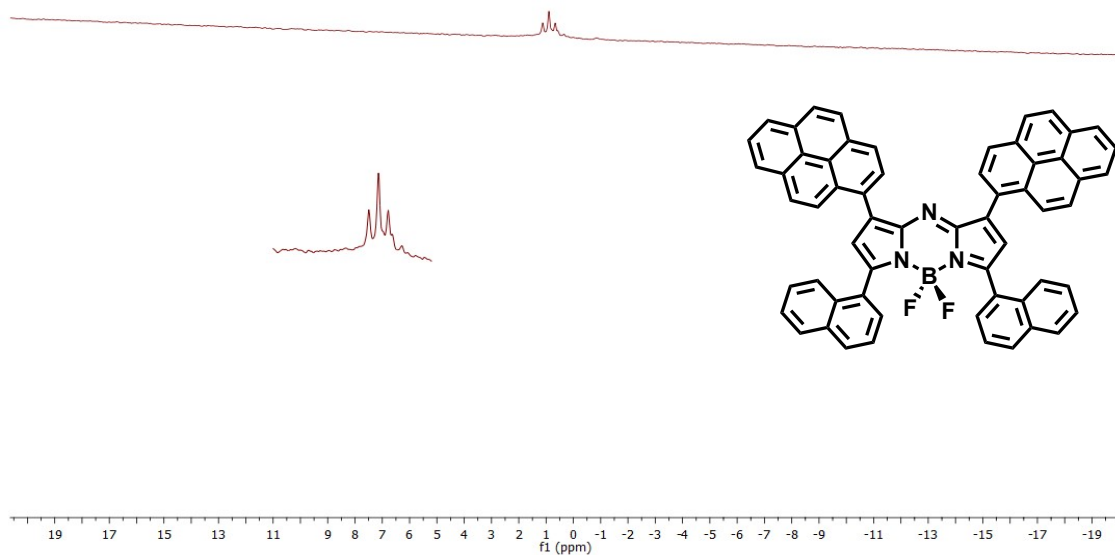


Fig. S17. ^{11}B NMR spectrum of 4,4-Difluoro-1,7-di (pyren-1yl)-3,5-di(1-naphthyl)-4-bora-3a, 4a, 8-triaza-s-indacene (**1**) in CDCl_3 .

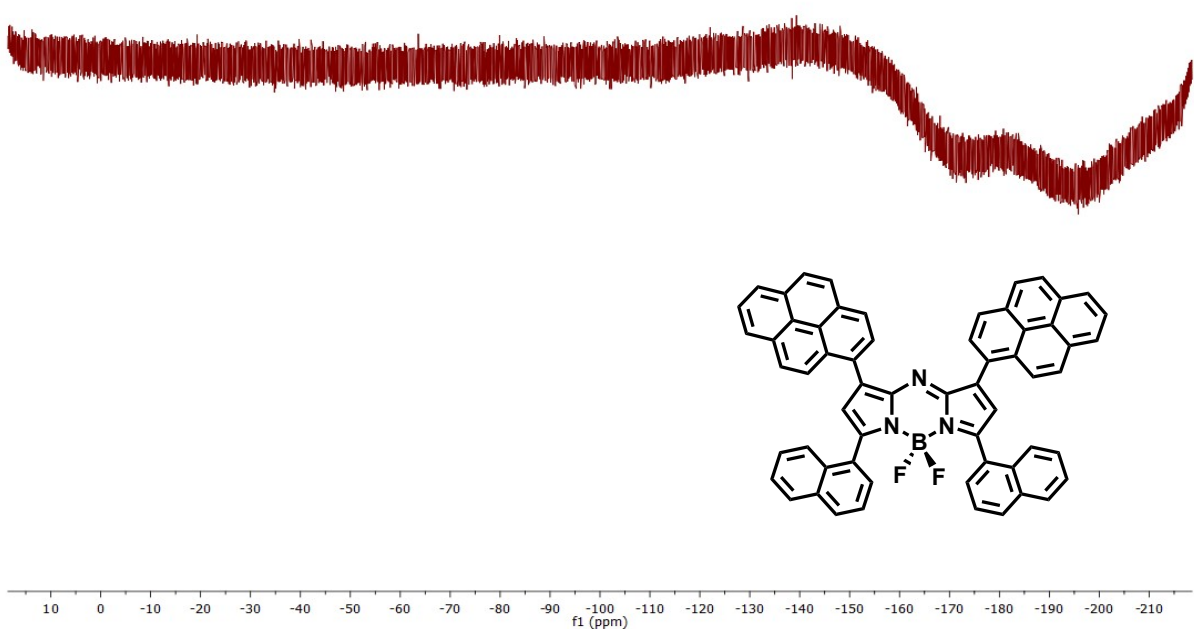


Fig. S18. ^{19}F spectrum of 4,4-Difluoro-1,7-di (pyren-1yl)-3,5-di(1-naphthyl)-4-bora-3a, 4a, 8-triaza-s-indacene (**1**) in CDCl_3 .

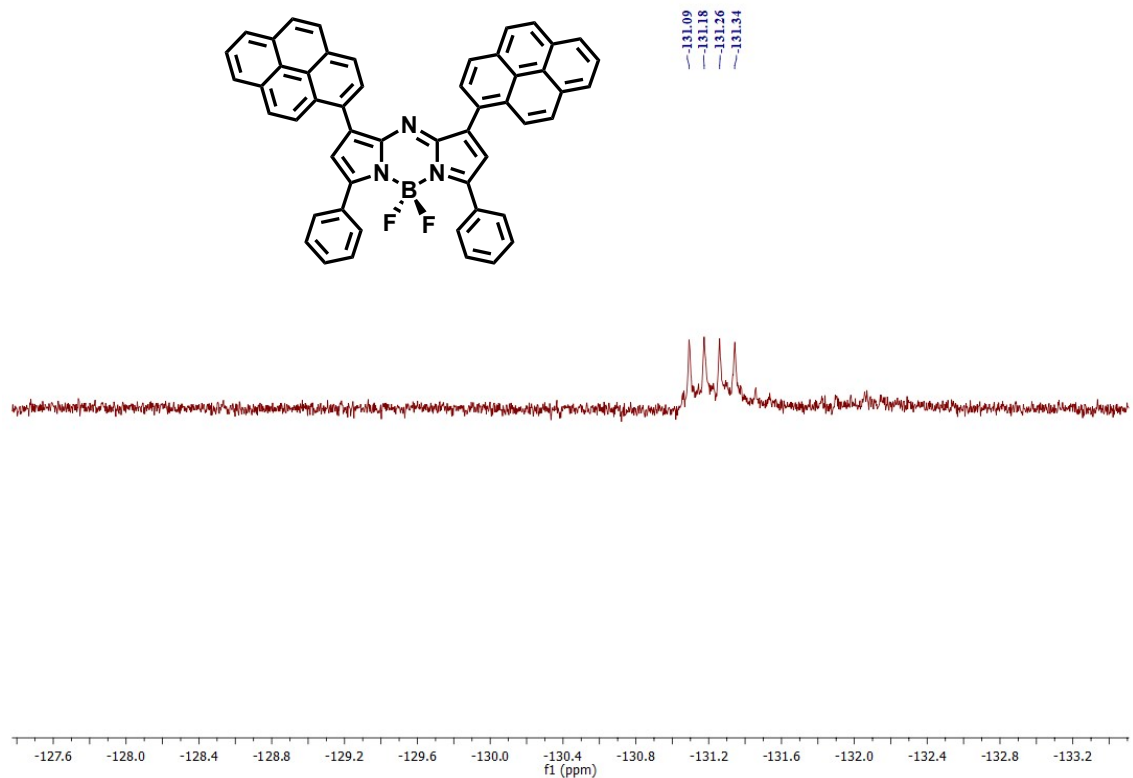


Fig. S19. ^{19}F NMR spectrum of 4,4-Difluoro-1,7-di(pyren-1-yl)-3,5-di(phenyl)-4-bora-3a,4a,8-triaza-s-indacene (**2**) in CDCl_3 .

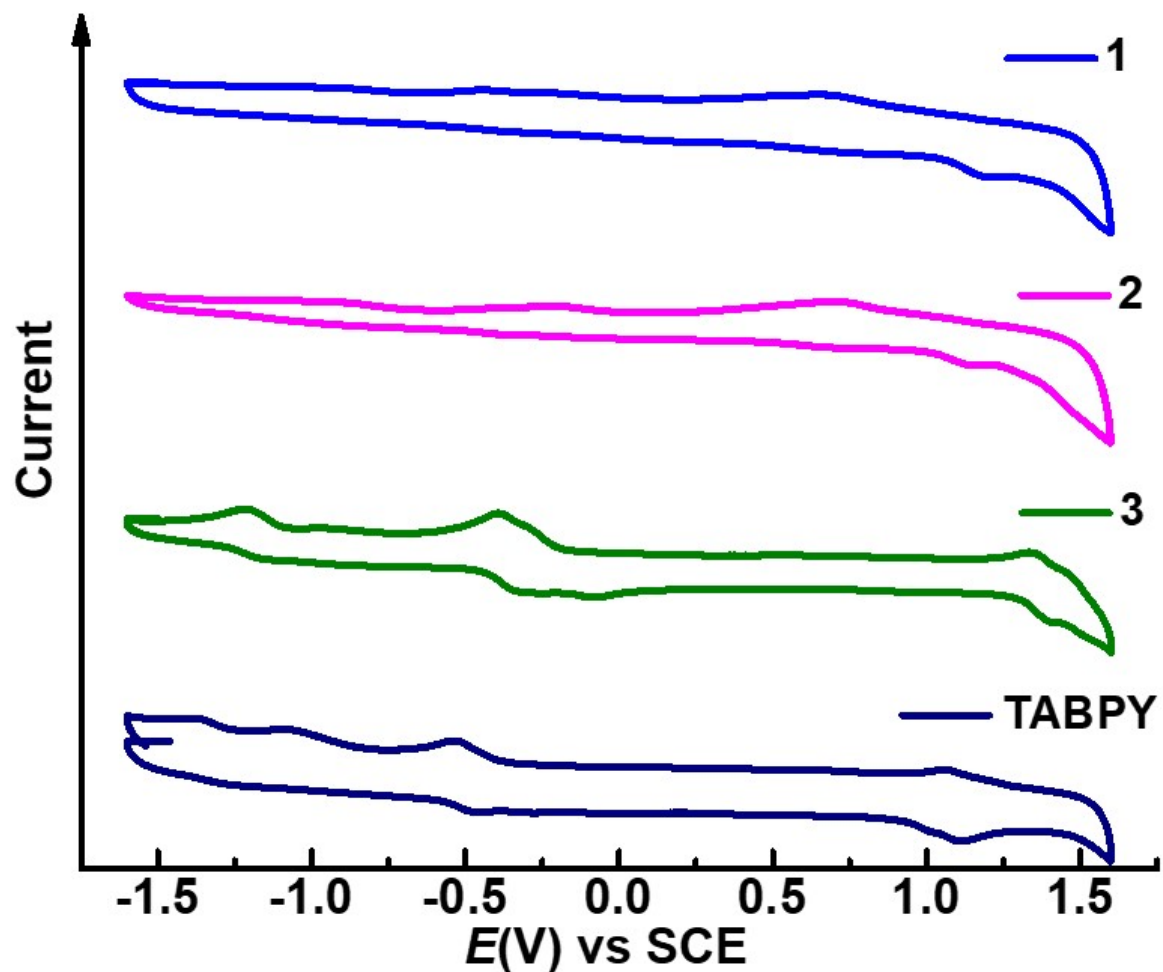
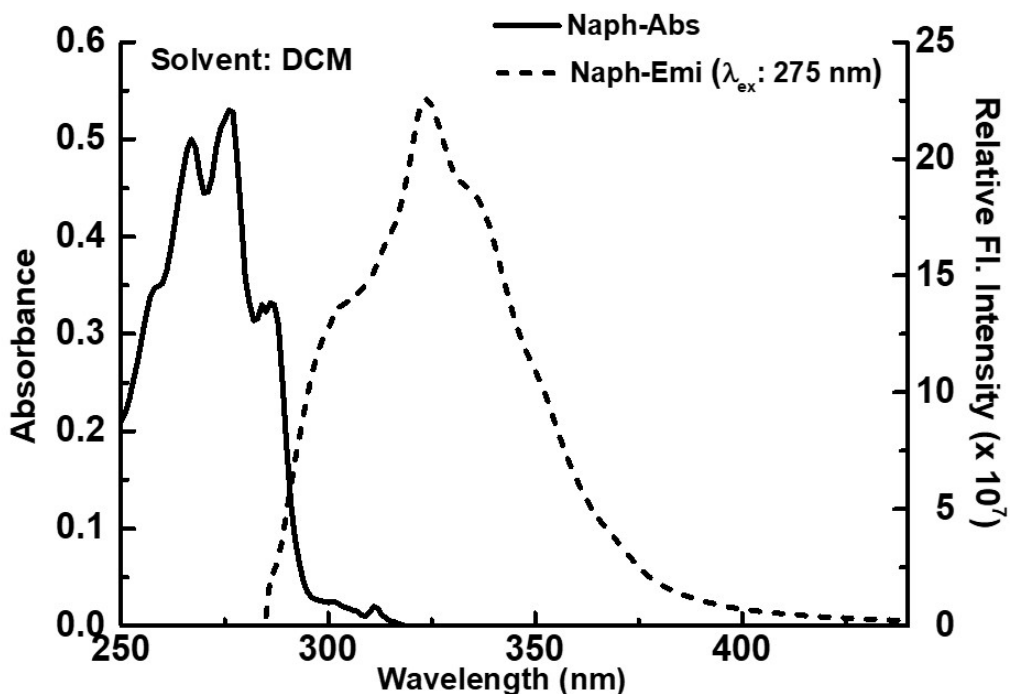


Fig. S20. Cyclic voltammetry of **1**, **2**, **3**, and **TABPY** in dichloromethane containing 0.1 M $(n\text{-C}_4\text{H}_9)_4\text{NClO}_4$, with the concentrations of the compounds held at 1 mM; scan rate = 20 mV s^{-1} .

(a)



(b)

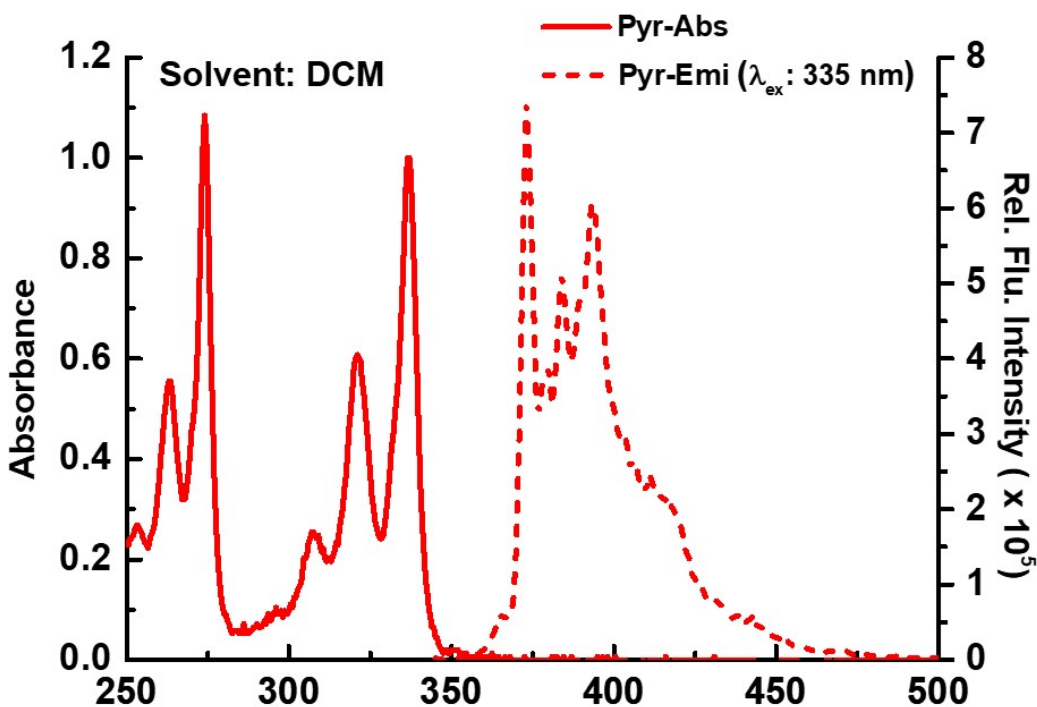


Fig. S21. Steady-state ((a) & (b) absorption and ((c): λ_{ex} : 275 nm & (d): λ_{ex} : 335 nm) emission spectra of **Naph** and **Pyr** in dichloromethane (DCM).

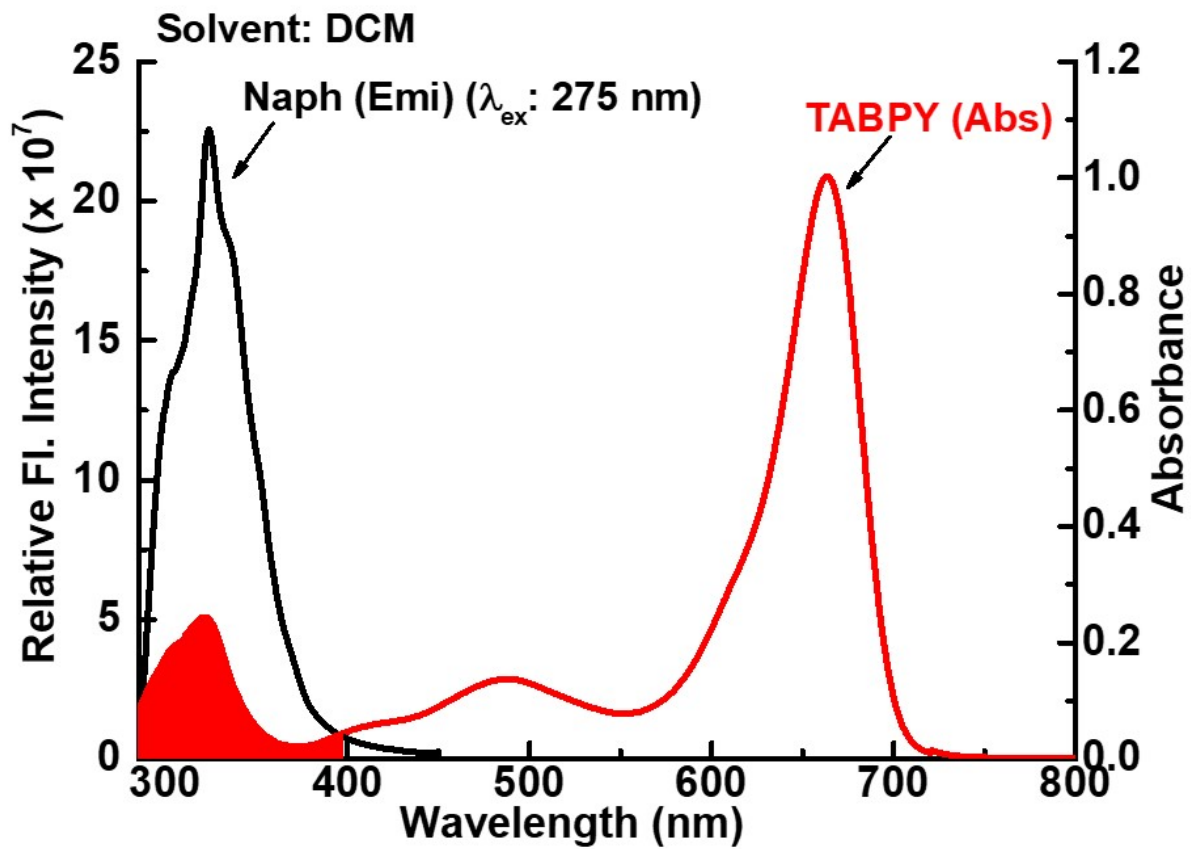


Fig. S22. Overlay of the steady-state emission spectrum of **Naph** and absorption spectrum of **TBAPY**.

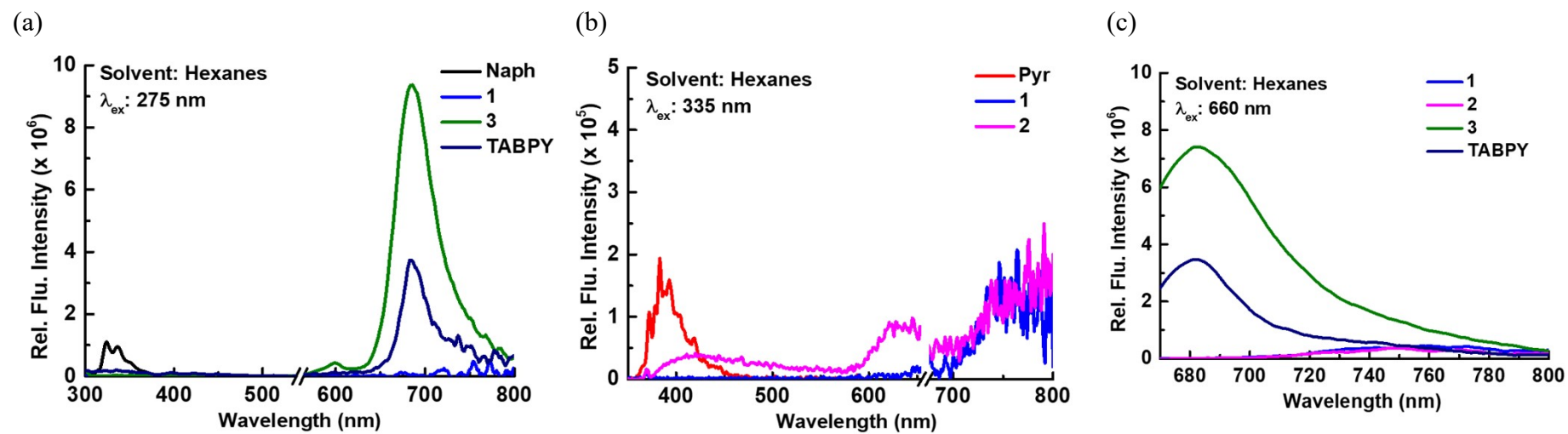


Fig. S23. Emission spectra of equiabsorbing solutions of **1**, **2**, **3** and the control compounds, **Naph**, **Pyr**, and **TABPY** in hexanes.

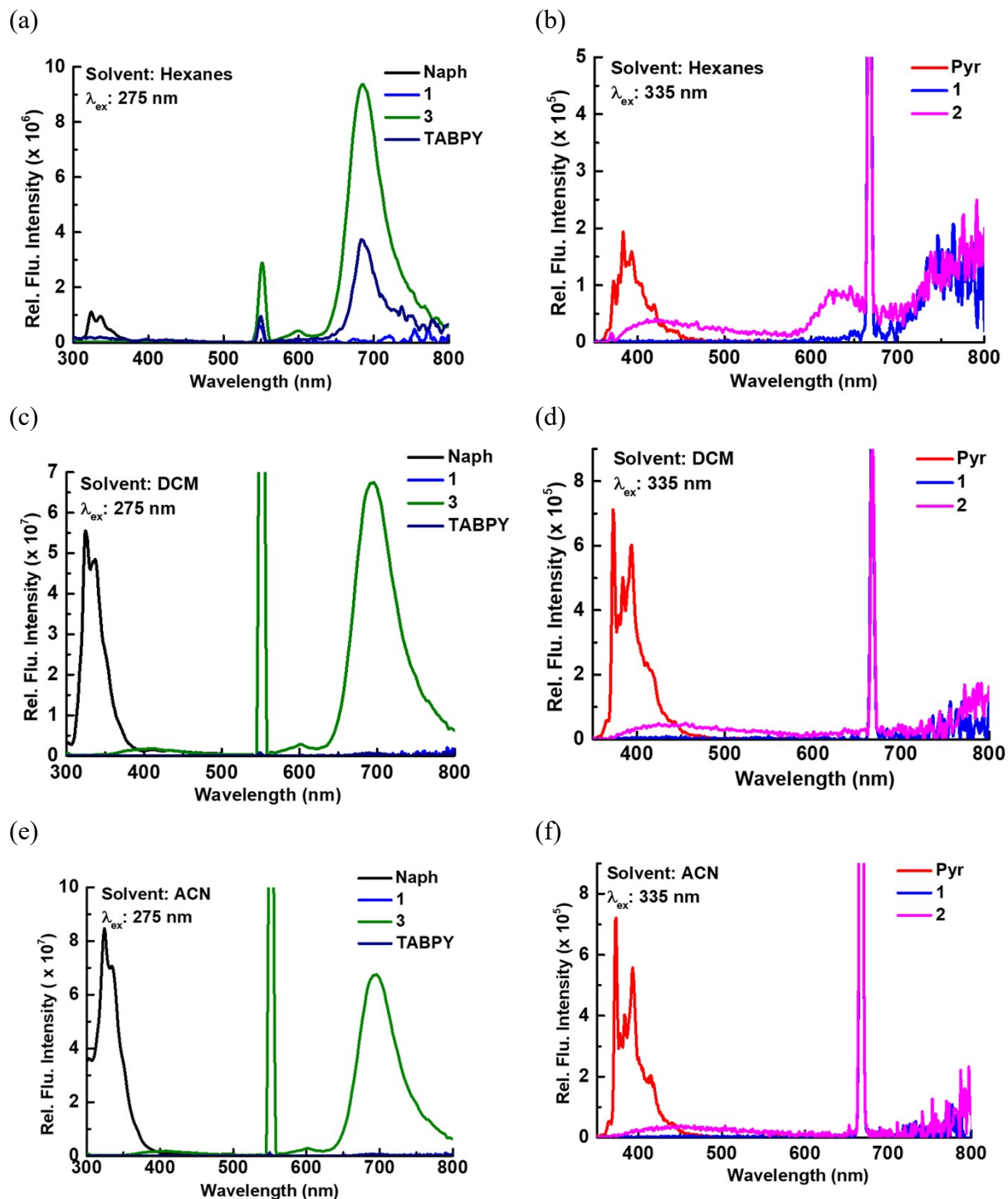
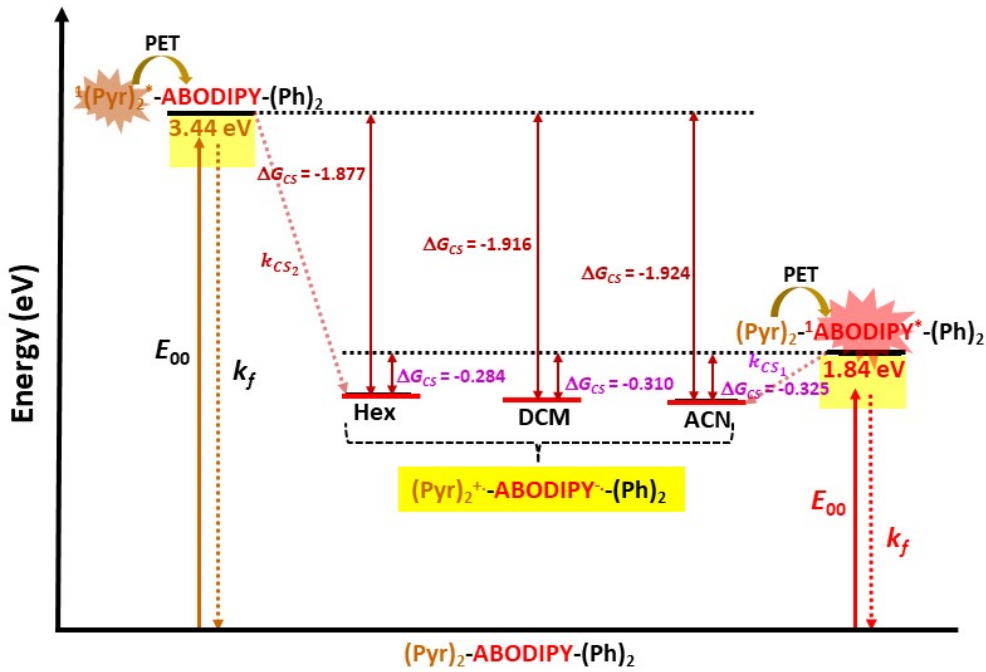


Fig. S24. Emission spectra of equiabsorbing solutions of **1**, **2**, **3** and the control compounds, naphthalene (**Naph**), pyrene, and 1,3, 5, 7-tetratolyl-azaborondipyrromethene (**TABPY**) in hexanes, dichloromethane (DCM), and acetonitrile (ACN) displaying the scattering peaks.

(a)



(b)

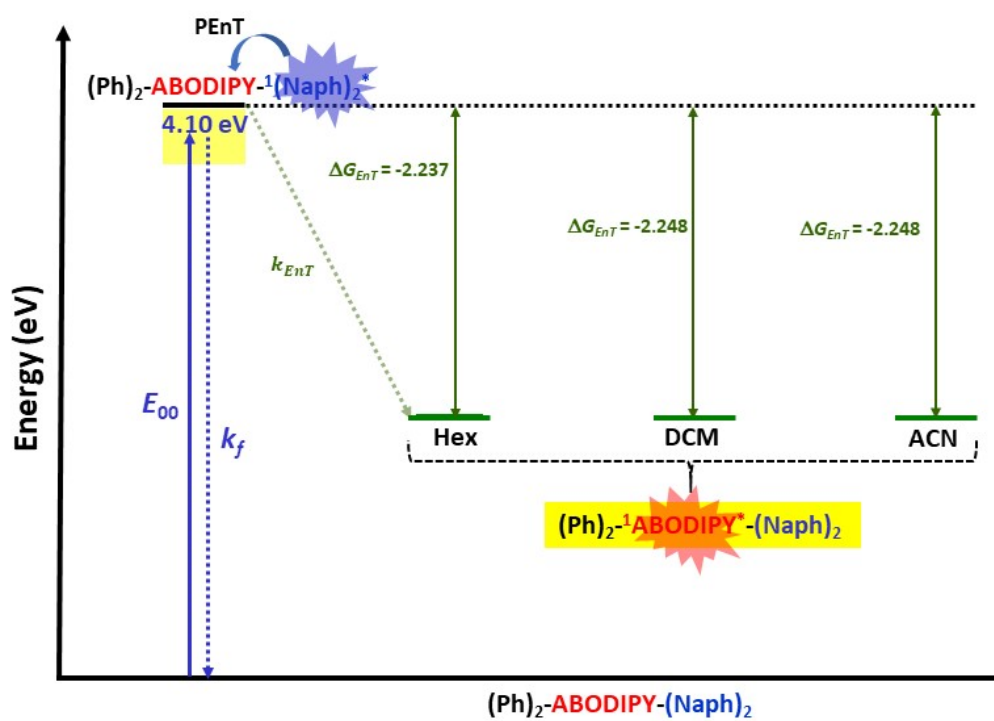


Fig. S25. Energy level diagram showing (a) photo-induced electron transfer in **2** and (b) photo-induced energy transfer in **3** in three solvents, hexanes, DCM, and ACN.

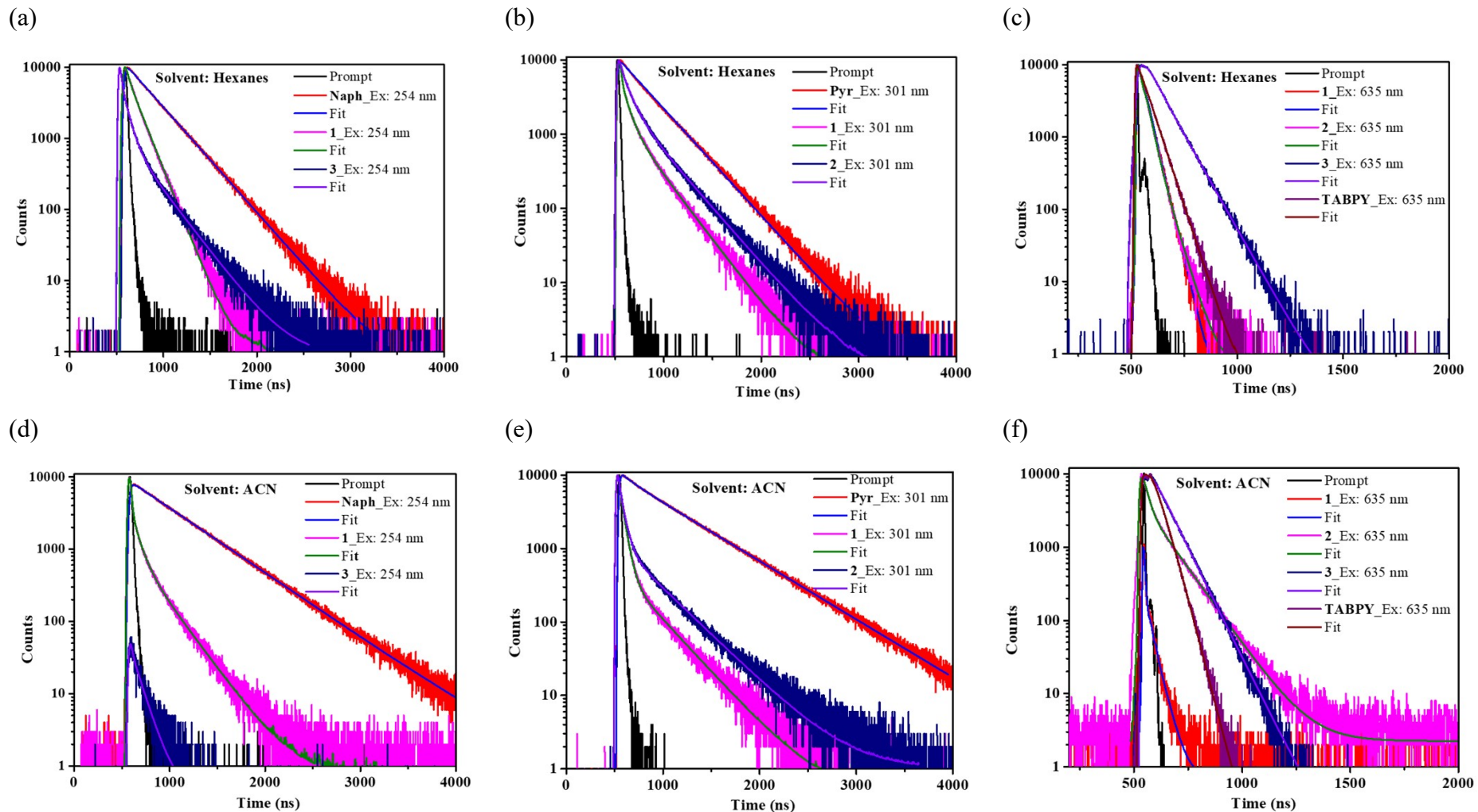


Fig. S26. Fluorescence decay curves of (a & d) naphthalene (**Naph**), **1**, and **3** ($\lambda_{\text{ex}} = 275$ nm), (b & e) pyrene, **1** and **2** ($\lambda_{\text{ex}} = 335$ nm), and (c & f) 1,3, 5, 7-tetratolyl-azaborondipyrromethene (**TABPY**), **1**, **2**, and **3** ($\lambda_{\text{ex}} = 635$ nm) in hexanes and ACN respectively.